

# Simulation of a heavily irradiated 3D silicon pixel detector

Giulio Bardelli

04 September 2019

Università degli studi di Firenze  
Supervisor Daniel Pitzl  
DESY summer student programme 2019

## Abstract

Silicon pixel detectors play an important role in trackers inside collider experiments such as CMS at LHC. It's already accepted that 3D pixels become more and more important and will replace the present planar pixel because of their properties. Being the first layers of the tracker it's necessary to understand their behaviour after radiation. After a brief explanation about 3D pixel technology, this report's aim is to compare the results which come from data with the ones provided by the model of a heavily irradiated sensor, focusing on the parameters that describe a sensor, such as efficiency and resolution used for tuning the parameters in the simulation.

## Contents

<b>1</b>	<b>Introduction</b>	<b>3</b>
<b>2</b>	<b>3D pixel sensor and their properties</b>	<b>3</b>
<b>3</b>	<b>Data analysis</b>	<b>5</b>
<b>4</b>	<b>Model of a heavily irradiated sensor</b>	<b>6</b>
<b>5</b>	<b>Comparison between data's results and model's results</b>	<b>9</b>
<b>6</b>	<b>Conclusion</b>	<b>12</b>

## 1 Introduction

CMS is one of the large experiments at LHC, CERN. This experiment is considered a general-purpose detector, so it is designed to reveal any kind of new physics phenomena, as happened for the discover of Higgs boson in 2012. In order to maintain this aim the detector is designed in the most general way possible regarding HEP detector, so with the classic onion structure. The first layers are trackers, which purpose is to give precise momentum vector of every charged particle's track in the collision, detected through semiconductor detector. Being really close to first collision, the tracker is heavily damaged by radiation. After the actual shutdown and a run in the same setting there will be a big upgrade for LHC machine, the so-called HL-LHC, which means high luminosity LHC. During this phase the number of events at the same collision, pileup, will increase and linked with that there will be an increase in radiation and in number of tracks. To succeed in detecting these new tracks it will be necessary to upgrade the detectors too. In the inner layer selection of events must be faster and for new sensors more granularity, more tolerance to radiation and a narrower pitch are required. A new kind of sensor, 3D pixel, was proposed in order to carry out these requests. 3D pixels are already produced and used in ATLAS, other detector at CERN, and now CMS groups are investigating their properties.

The purpose of the work, reported here, is to create the first model which can reproduce the behaviour of one of these sensors after being heavily irradiated in order to have a comparison with data. Data that are actually analysed inside this report. Having a simulation can also help to understand some differences in sensors' pitch and how these affect the result (  $50 \times 50 \mu m$  or  $100 \times 25 \mu m$  are distinct prototypes). A hopeful aim could be the chance to forecast the behaviour of these pixels for future measurements in various conditions so as to understand if they can successfully replace present sensors and how long can they be efficient in CMS phase II (HL).

## 2 3D pixel sensor and their properties

Semiconductor detectors are already well-known for their properties such as granularity, high spatial resolution, fast collection of charge, etc. Nowadays almost every tracking system is based on these devices, especially on doped silicon ones, which has the advantages of being present in large area and being fast at collecting charge. The first detector conceived with silicon was a strip detector, where charge was collected by microstrips implanted in silicon, and which needed two layer rotated to have 2D information, mandatory for the coordinates of the tracks. Thanks to their good spatial resolution and to a different readout electronics, which is separated for each pixel and connected to them through bump bonding, the next generation of silicon detectors, the hybrid pixel sensor, easily replaced the microstrip ones in the inner layer of the tracker in most experiment. Despite that, for example, in the outer tracker of CMS there are microstrip sensors.

Another step made in order to improve the reconstruction of tracks is the introduction of 3D pixel, instead of planar ones. The main difference in geometry, which then affects properties, is that in a planar device we have two oppositely doped layer, one on the top, and the other on the back, whereas in 3D pixel we have  $n^+$  and  $p^+$  doped columns etched into silicon. The convention (n over p or p over n) depends on where the bump bonding is put, and to preserve the electronics, the connection is with the  $n^+$  doped columns, which are at ground, whereas the  $p^+$  ones are connected to a negative voltage. In that way the volage difference allows the depletion inside the sensor, so the creation of holes and electrons while a charged particle passes through. This difference in geometry leads to differences in resolution and above all in efficiency, which is linked to the mean free path of the electron,  $\lambda_e$ , and to the distance that charge carrers have to travel in the sensor,  $L$ , trough this formula  $SE = \frac{1}{1+0.6\frac{L}{\lambda_e}}$ . From this formula it's clear that reducing  $L$  increases the signal efficiency,  $SE$ , and it's possible to realise this fact in 3D pixel configuration, as it's shown in Figure 1.

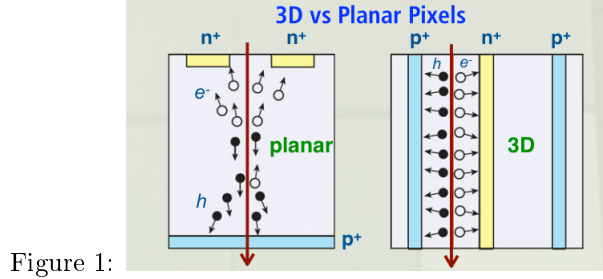


Figure 1:

Other advantages given from 3D pixel are the faster collection of charge, the lower bias voltage needed to deplate the region inside the semiconductor and the higher collected charge due to less trapping. Obviously there are some disadvantages, such as less charge charing, some low field region or inefficent region (electrodes) and an higher cost. Nevertheless it's already planned to replace planar pixel with 3D pixel in the first layer of the inner tracker inside CMS, and there is a discussion about second and third layer.

The parameters that describe a silicon detector are efficiency and spatial resolution, important for the reconstruction of tracks, but it's necessary to take other two parameters into account, which are the charge sharing and the tolerance for radiation. The first is related to spatial resolution and is heavily dependent on geometry, whereas the second one is important to maintain the detector's properties unchanged in time. 3D pixels show an high radiation's tolerance, in fact also being heavily irradiated (order of  $10^{16} \frac{n_{eq}}{cm^2}$ ) they preserve an high tracking efficiency. Despite of the giant steps made in this direction, radiation remains still a big issue for HEP detectors and that's why must be included in the simulation.

### 3 Data analysis

Firstly, in order to have a model of the 3D pixel, it's necessary to analyze data taken from an irradiated sensor and to understand them. The device under test is a FBK 3D, with dimension  $50 \times 50 \times 130 \mu m$ , interconnected with a RD53A read out chip, both heavily irradiated at Cern with a fluence of  $10^{16} \frac{n_{eq}}{cm^2}$  and then analyzed on April at DESY test beam, with MIMOSA telescope. This kind of telescope is made of six silicon planes and the reconstruction of tracks goes by triplets, ahead the DUT and after this one. Eudaq, from DAQ, is the software used for taking data and then these are offline analyzed by EUTelescope, which works through iterations and it's divided into two parts. The first is "tele", which provides the alignment of the telescope's planes, the hot pixels of these ones and a map of the charge collected by the DUT, in order to mask it removing hot pixels. Instead the second one, "scope53m", is responsible for the alignment of the DUT and the alignment of MOD, a reference module necessary for resolved position and fast timing, because telescope itself has an integration time order  $100 \mu s$ .

The first measurement was done with vertical efficiency in order to have a curve efficiency vs different bias voltage (from -40 to -170 Volt), then bias voltage was fixed at -170 volts and the sensor was turned to have various resolutions at distinct angles. The efficiency in this case was always above 99% because of the fully depletion of the sensor and it's relevant to consider the charge sharing between pixels which helps in reconstructing track, removing uncertainties in coordinates due to single pixel (box error  $\frac{width}{\sqrt{12}}$ ).

First useful result is the efficiency plot, which is shown below in Figure 2. From this plot we can clearly understand that the 3D pixels, although irradiated, are still efficient also going at medium-high bias voltage and then this curve reaches an asymptotic value, in which efficiency is 99 % while increasing bias voltage. It's also shown that in very low bias voltage the efficiency is far less than 90%, because of the low field region between electrodes. It's helpful to remind that the same efficiency is reached in planar pixels with bias voltages three times higher. Figure 3 shows the resolution versus the angle. As it's clear from it, the best resolution in spatial position is at 20 degrees, while the resolution gets a lot worse with high tilt angle. In data residual are fitted with a generalized exponential function into three sigma and once obtained this residual it's important to subtract to it the contribution of the telescope, which can add a systematic error of  $2 \mu m$ . The data for this scan were taken in two configurations, one for high turn angles and the other one for small turn angles, which differ for dissimilar amount of insulating material, amaflex, between MIMOSA's planes and the DUT. This fact lead to an unforeseen correlation between angle and resolution in y, the direction which should be independent of angle, in telescope's configuration. It's possible to use this correlation to correct data through data but despite of taking in account that in higher angles the resolution is still a bit worse.

From data's plots of efficiency it's also possible to learn a lot about the collection of charge in an irradiated sensor and then these information are useful

Figure 2:

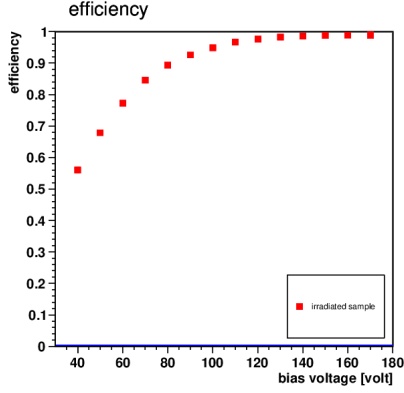
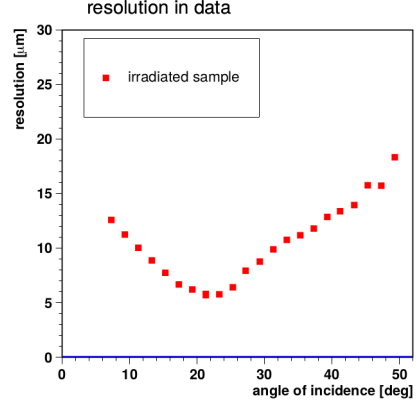


Figure 3:



to reproduce charge's density inside the model. The distribution of collected charge varies from high and low bias voltage, as it's shown in plots below. In Figure 4, at -80 Volt, the distribution looks like a cloverleaf function and the charge is not collected in low field region between electrodes, whereas in the second plot, at -170 Volts, the charge is more confined in the center, where there is the read-out electrode, leaving electrode's corners as less efficient regions. It's relevant to point out the difference between the two scales of efficiency : first one starts from 0.75 and the other one, at higher voltage, starts from 0.965.

Figure 4: 80 Volt

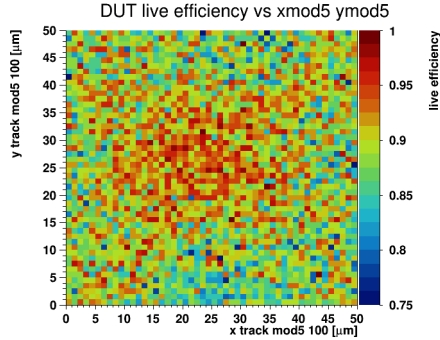
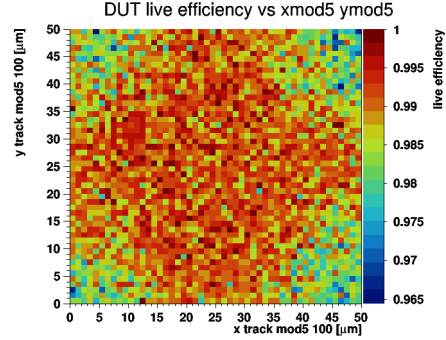


Figure 5: 170 Volt



## 4 Model of a heavily irradiated sensor

The model used for simulating data comes from KDetSim, a shared library based on root and on its commands, which can solve Poisson equation and deal with the charge transport inside a semiconductor detector through Monte-Carlo

simulations. The representation starts with a single 3D pixel,  $50 \times 50 \times 120 \mu m$ , unirradiated with just one read-out electrode in the middle of the sensor, an example taken from KDetSim's library. The best way to update this example and make it closer to data it's proceeding by steps, so as to verify how each contribute influence the model.

First it's important to find a mathematical function which can describe the charge density inside the sensor. Observing data's plots of efficiency it's clear that this function must be confined in the center for higher voltage and then becomes a cloverleaf if bias voltage's absolute value is lower. A function that could describe this behaviour has to be divided in an exponential part, quadratic in x and y or not, and in a part which should depend on polar angle and should provide this cloverleaf's shape. Nevertheless this function has to be integrable to allow the solution of Poisson equation with periodic boundary condition. After some attempts, the choice was  $Q \times \exp(\frac{(y-y_0)^2 + (x-x_0)^2}{\delta^2}) \times (\frac{(y-y_0)^2 + (x-x_0)^2}{\delta^2} \sin(2\phi) + P2)$ , where  $\phi$  is defined as  $\frac{y-y_0}{x-x_0}$ . Therefore Q, P2 and  $\delta$  become parameters in the simulation whom is manageable to fix through the constraints given from data or to pursue physical reasons. The plot, Figure 6, shows the result in collected charge for the model at -170 Volt.

Figure 6:

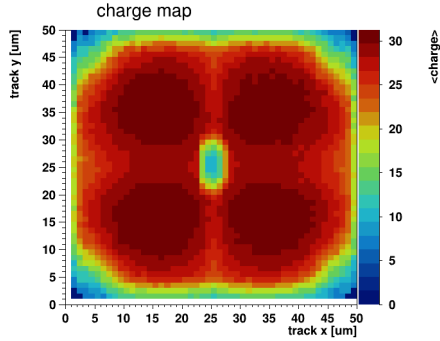
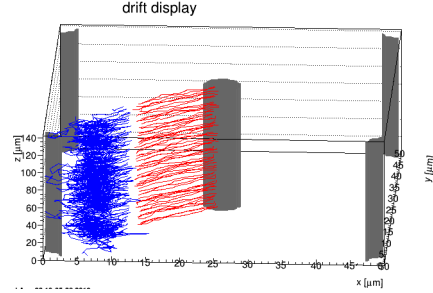


Figure 7:



In order to be close with reality considering an irradiated pixel, it's also important to add trapping at the model, because holes and electrons can be trapped due to defects in valence band, or can produce leakage currents and latest the sensor collect less charge. This effect is dominant for low voltages, whereas it's a second order effect for high voltages. In KDetSim medium lifetimes for electrons and holes in silicon,  $\tau_h$  and  $\tau_e$ , are defined and allow adding trap; in this model they are linked to irradiation fluence, known from CERN, and to  $\gamma_h$  and  $\gamma_e$ , which are estimated from previous analysis in planar pixels, through this formula  $\tau_{e/h} = \frac{1}{fluence \times \gamma_{e/h}}$ . In Figure 7 there is shown trapping's effect in holes drift for -80 Volt.

Then it's relevant to have more than one pixel to predict the behaviour of resolution at different angle and to control the charge sharing between pixel for

all available turn angles (from 6 to 48 degrees). For this reason while looking at pixel's dimension it's helpful to quadruplicate the model along one direction, in order to contain at least all angles inside the model and to discuss the cluster size, which is the number of pixel above threshold linked by same track, in each case. Looking at how the model is done it was decided to increase y dimension, so turn angles in the rapresentation will be replaced by tilt angles. In order to contain every tilt angle the dimensions of the model changed to 50x200x142  $\mu m$ , and space charge must be repeated in each pixel. Dealing with defined boundary conditions in KDetSim it was clear that the electric field on z direction was completely unphysical, so these conditions had to be changed in periodic ones. Although that it still remains some correlation between the thickness and the minimum in resolution. To overcome that, thickness was increased in order to not take in account some border effects and to displace the minimum in resolution in the right direction. What also allows this way of proceeding is the fact that the sensor is not 130 micron thick, but this one is only the active area and there is some more materials at the back which can alter collected charge. The field in this configuration is shown below in figure 8.

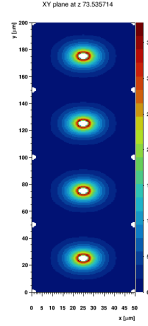


Figure 8:

At the end it's compulsory consider not only the geometry and the field but also the readout electronics and the digitalization of the signal, which arrives as analog but after the discriminator is a digital signal, in order to be processed by computer logic. First parameter that must be added at the model is the threshold, thinking about the fact that the tracker detector are the first selectors in a HEP experiment and threshold is a lot influent on cluster size. Then it's relevant to take in account that the digitilazion of signal happens through a "Krummenacher" shaper after a preamplifier. This shaper works with the Time over Threshold system (ToT) and with only four bins to make the read out process faster, so it can digitalize the signal into sixteen values and the last one represents the overflow. The ToT system can provide this trasformation to digital, in order to send information at the CPU logic, in a simple way. It mantains costant the slope while the capacitor is discharging and knowing this slope, knowing when the signal reach the capacitor ( $t_0$ ) and receiving from there the amplitude's raising can estimate the difference in time and then divide it by sixteen to obtain the correct digital value. In figure 9 there is a scheme on how



ToT works. What's more the response of each preamplifier is slightly different, so there is the necessity to have a gaussian smearing for the ToT value that scales the model to digitalize the charge. To be consistent with reality another physical phenomenons that take place in the semiconductor detector are delta rays, namely low energetic electrons produced in a second or third interaction, and not by the first high energy particles that come from the collision in accelerator. These electrons contribute to the curve of charge collected in sensor, which should be a gaussian, adding a Landau tail. At the end there's also the noise due to the read out chip connected to sensor, which is simply modeled as a gaussian smearing around the mean value, that is actually the charge in each single pixel before the digitalization. There could be taken in account also the cross-stock, which is the coupling between diodes seen as capacitors, but this effect affects a lot cluster size displacing it from the value in data. All these effects are shown in the total charge plot at  $37.3^\circ$  ( Figure 10).

Figure 9:

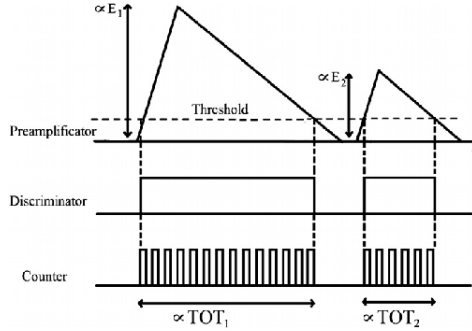
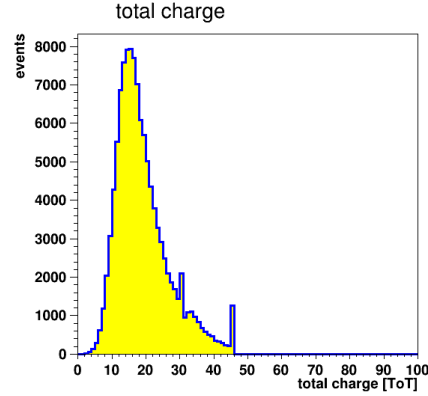


Figure 10:



## 5 Comparison between data's results and model's results

Once having elaborated the model it's necessary to tune parameters with data's constraints in order to reproduce the same results or to have some behaviour's reference that should be expected from data. Constraints can come from physical observables analysed in data or in order to maintain physically reasonable the model; for example that happens for the variables in the formula for irradiated density charge. In fact  $P_2$  and  $\delta$  are fixed to avoid region in the model where potential is greater in absolute value than bias voltages, which is a violation of boundary conditions whereas space charge (  $Q$  ) is tuned to reach same efficiency as data at the same voltage. This comparison is good at high bias voltages, whereas it doesn't work so well in lower voltages where if space charge

is pushed to reach same efficiency as data boundary conditions arise violated. That it's shown in Figure 11 below. Figure 12 shows the relation between space charge and bias voltage, which unexpected seems to be linear. Fitting that with a polynomial function gives a slope of  $3.82769 \mu m^{-3} V^{-1}$  that could make the model more dynamic removing a parameter dependent on physical quantity (space charge) to add a global parameter, such as the slope.

The Figure below are obtained in this configuration with a single pixel in a vertical incidence but, when looking at the four pixel configuration, it happens that space charge affects a lot the position of the minimum in resolution. Working at 170 Volt this parameter should be  $670 \mu m^{-3}$  but in order to avoid this displacement it is fixed at  $600 \mu m^{-3}$ . That is justifiable because the model is not very sensitive between 100 % of efficiency and 99 % of same quantity. Instead of that the representation is really sensitive at medium-low voltages when the efficiency is a lot different from 100%.

Figure 11:

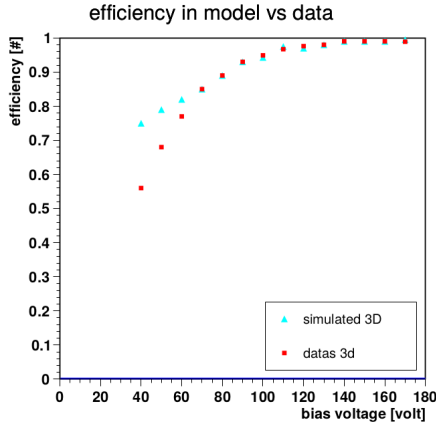
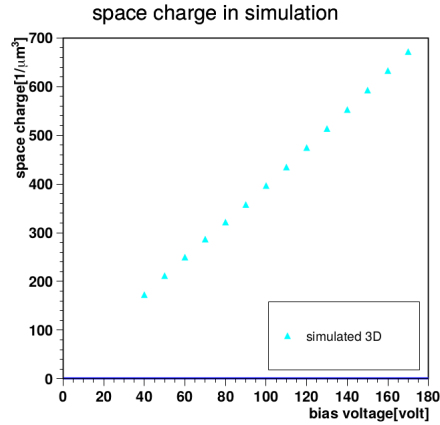


Figure 12:



Other parameter that needs to be fixed looking at data's constraints is the ToT scale in order to have same distribution of charge in central pixels, the ones which experienced more the charge sharing, with data one. This ToT scale's value is fixed at 0.7 while Landau's fluctuations are on, and at 1.8 if Landau's fluctuations are off. In Figure 13 it's shown the number of cluster size at different value of charge (ToT units) in data at 21.3 degrees. The comparable quantity in the model is the number of events in which each pixels charge is above threshold at the same angle, Figure 14. To make this plot clearer it's remarkable to say that blue and black colours refer to central pixels, while red and green refer to external pixels. Looking at these two first figure the trend is similar, they are both dominated by overflow value of charge (15) and they don't show linked pixels below threshold. Plotting the same quantity at a different angle it's possible to see the same behaviour of data and model but different results, as it's done in Figure 15 and 16 having an angle of 45.3°.

In this case the pixel below threshold are normally suppressed but it's useful to point out that the number of overflow is decreased, consistently with increasing the angle, so the cluster size. That actually means that the charge is the same, but it's divided between more pixels, instead of being in just one pixel as it happens at 21.3°.

Figure 13: data 21.3°

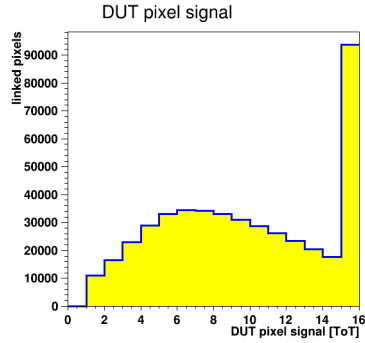


Figure 14: model 21.3°

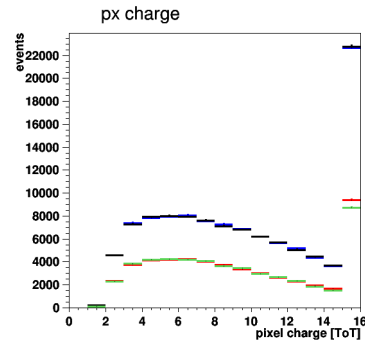


Figure 15: data at 45.3°

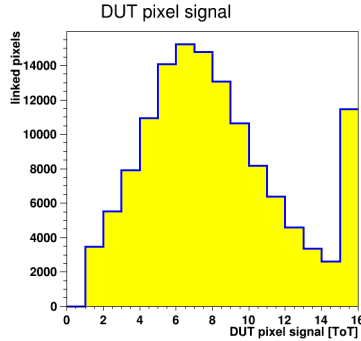
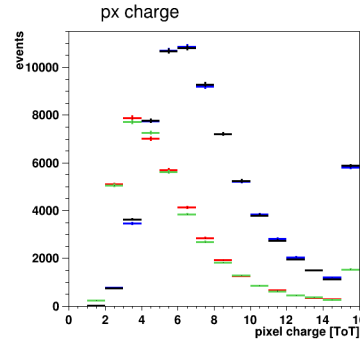


Figure 16: model at 45.3°



Threshold can be setted looking to another physical constraint, such as the cluster size, remembering that threshold is a global parameter equal for every pixels and applied at all of them. In the model is setted at 1.7 ke, so as to have same cluster size in model and in data at the optimum resolution. It's expected that cluster size will increase with the angle because this quantity is proportional to the tangent of this angle. Once fixed the threshold it's possible to obtain cluster size for every tilt angles and to match them with data's result; with the value setted before it's possible to describe quite well the general trend of this curve, as it's shown in Figure 17. Everything is fixed and it's possible to analyse the resolution of the model at different angles as shown in Figure 18. First is important to notice that data are well described at optimum of resolution and at low angles with systematic error introduced by telescope. Then it's also clear that there is a big discrepancy at higher angles that could be caused by

some artificial problem hidden in the simulation but could also be caused by this difference in MIMOSA telescope configuration for the two different scan made in April. In the 3D irradiated model it's also possible to see that there is another minimum around 40 degrees, also if it is smeared by noise. This minimum should be expected by geometry, because it's linked to the width of pixels and 40° is the tilt angle in which the tracks hit three pixel instead of two ( same reason to expect a minimum at ~20°). Despite that in data the bad resolution covers the second minimum.

Figure 17:

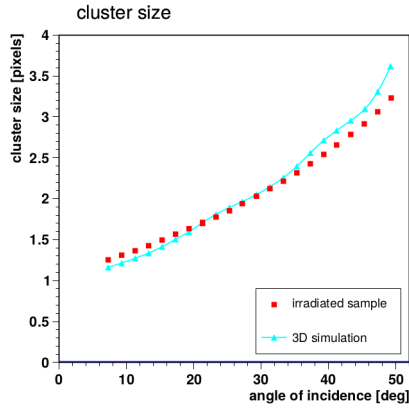
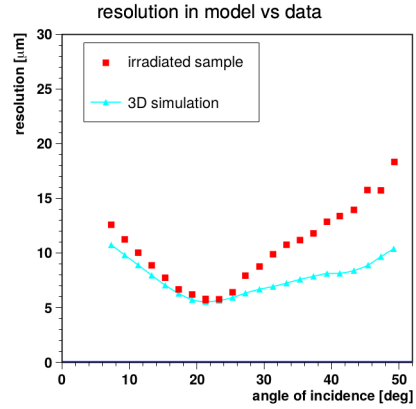


Figure 18:



## 6 Conclusion

In order to sum up this report the most important things to take in account are the resolution's and efficiency's analysis, whence it's possible to derive interesting result for 3D pixel, such as the high efficiency over 130 Volt or the optimum resolution at 6  $\mu m$ . These values must be pointed out to show the good properties of 3D pixel after being heavily irradiated. The other interesting thing could be this model which is the first for a 3D irradiated pixel and has this function for space charge density inside the sensor. What's more this representation can describe the gross feature of data, especially in minimum of resolution while the bias voltage is high, although some discrepancy at extremes. This simulation could be improved tuning differently some parameter but the main idea to improve that is taking more data of the sample with different fluences, that could be a future plan to better understand how 3D pixels behave after radiation.

## References

- [CERN-LHCC, 2017] CERN-LHCC, 09-2017. *The Phase-2 upgrade of the CMS tracker*
- [Gregor, 2019] Gregor Ingrid-Maria, 2019. *Lecture in HEP detectors* during 2019 DESY summer school in DESY indico agenda.
- [Duarte-Campderros,2019] Duarte-Campderros J. on behalf of the CMS collaboration, 2019. *Result on proton-irradiated 3D pixel sensors interconnected to RD53A readout ASIC*. <https://doi.org/10.1016/j.nima.2019.162625>.
- [Dreyling-Eschweiler, 2018] *Dreyling\_Eshweiler Jan et al., 2018. The DESY II test beam facility.* <https://doi.org/10.1016/j.nima.2018.11.133>.
- [Jansen, 2016] Jansen Hendrik et al., 2016. *Performance of the EUDET-type beam telescopes*. EPJ Techniques and Instrumentation volume 3, Article number: 7.
- [Kramberger, 2012] Gregor Kramberger, 2016. *KDetSim reference guide*. [https //kdetsim.org](https://kdetsim.org) .